

## Fast switchable electrochromic properties of tungsten oxide nanowire bundles

Sung Jong Yoo, Ju Wan Lim, and Yung-Eun Sung<sup>a)</sup>

School of Chemical and Biological Engineering, Seoul National University, Seoul 151-742, Korea and Research Center for Energy Conversion and Storage, Seoul National University, Seoul 151-742, Korea

Young Hwa Jung, Hong Goo Choi, and Do Kyung Kim

Department of Materials Science and Engineering, Korea Advanced Institute of Science and Technology (KAIST), 373-1 Guseong-dong, Yuseong, Daejeon 305-701, Korea

(Received 14 February 2007; accepted 4 April 2007; published online 27 April 2007)

The authors prepared uniformly shaped  $\text{WO}_{2.72}$  nanowire bundles using the solvothermal synthesis method. They investigated the potential of the  $\text{WO}_{2.72}$  nanowire bundles to be used as a cathode electrode for electrochromic devices and the effect of the  $\text{Li}^+$  insertion (or extraction) kinetics and diffusion of  $\text{Li}^+$ . An electrode consisting of arrays of  $\text{WO}_{2.72}$  nanowire bundles was formed and used in an experiment using the Langmuir-Blodgett technique. The one-dimensional nanostructure of  $\text{WO}_{2.72}$  has a high Li-ion diffusion coefficient ( $\sim 5.2 \times 10^{-11} \text{ cm}^2/\text{s}$ ) and low charge transfer resistance ( $\sim 28.6 \Omega$ ), which result in its having a fast electrochromic response time (coloring time  $< 3.5 \text{ s}$ , bleaching time  $< 1.1 \text{ s}$ ), and outstanding high coloration efficiency ( $> 55 \text{ cm}^2/\text{C}$ ). © 2007 American Institute of Physics. [DOI: 10.1063/1.2734395]

Electrochromic (EC) devices which make use of the phenomenon of electrochromism, wherein the color changes depending on the potential of an applied electric field, have many potential applications such as smart windows, mirrors, and eyewear, as well as in EC displays such as mobile phones, smart cards, and price labels,<sup>1</sup> due to their low power consumption and high energy efficiency.<sup>2-4</sup> Tungsten oxide remains the most extensively studied electrochromic compound and the most promising candidate for EC devices. However, this material fails rapidly, owing to the dissolution of the film in the acid solution employed in EC devices; therefore, to avoid the use of acid, it has to be used in a  $\text{Li}^+$  based electrolyte, but this results in a slower electrochromic response (ER) time ( $> 10 \text{ s}$ ).<sup>5</sup> The ER time of tungsten oxide in a  $\text{Li}^+$  based electrolyte is limited by the lower diffusion coefficient ( $D_{\text{Li}^+} = 2.4 \times 10^{-12} - 2.8 \times 10^{-11} \text{ cm}^2/\text{s}$ ) of  $\text{Li}^+$  into the film during the insertion/extraction process and may limit its application to EC windows only.<sup>6</sup> The ER time of an EC device is mainly affected by factors such as the ion diffusivity in the cathodic and anodic coloration materials<sup>1</sup> and the electric resistivity of the transparent conducting layer.<sup>7</sup> The ion diffusivity in the coloration materials is the more important factor in determining the ER time of an EC device. The simplest way to overcome the slow ER time is to decrease the diffusion distance of the ions by decreasing the electrochromic film thickness [ $d \approx \sqrt{D_{M^+}(ER)}$ :  $d$  = thickness].<sup>8</sup> However, the coloration of such a thin film made by the sputtering method is insufficient for electrochromic applications (e.g.,  $\Delta\text{OD} = 0.16$  and  $\text{ER} = 2 \text{ s}$  for a film thickness of 40 nm). One approach to achieve these properties is the use of one-dimensional (1D) nanostructures (nanowires, nanorods, nanotubes, etc.).

Recently, 1D nanostructured semiconductor oxides, such as  $\text{CuO}_2$ ,<sup>9</sup>  $\text{TiO}_2$ ,<sup>10</sup>  $\text{ZnO}$ ,<sup>11</sup>  $\text{SiO}_2$ ,<sup>12</sup>  $\text{VO}_2$ ,<sup>13</sup> and  $\text{WO}_x$ ,<sup>14,15</sup> were reported. Although there have been some reports on the synthesis of tungsten oxide 1D nanostructures, there has been little research into their electrochromic properties. Herein,

we report the electrochromic properties of tungsten oxide nanowire bundles synthesized using the solvothermal method. In addition, we applied the Langmuir-Blodgett (LB) technique to produce arrays of the synthesized tungsten oxide nanostructures on a large scale and investigated the electrochromic properties of the 1D tungsten oxide LB films. A LB method is the technique to obtain 1 ML of an organic/inorganic material deposited from the surface of a liquid onto a solid by immersing the solid substrate into the liquid.<sup>16</sup>

1D nanostructure tungsten oxide bundles were synthesized via a simple solvothermal method. The detailed synthesis process is described in our previous paper.<sup>15</sup> Figure 1(a) shows the transmission electron microscopy (TEM) micrographs of the  $\text{WO}_{2.72}$ -NBs ( $\text{WO}_{2.72}$  nanowire bundles) which

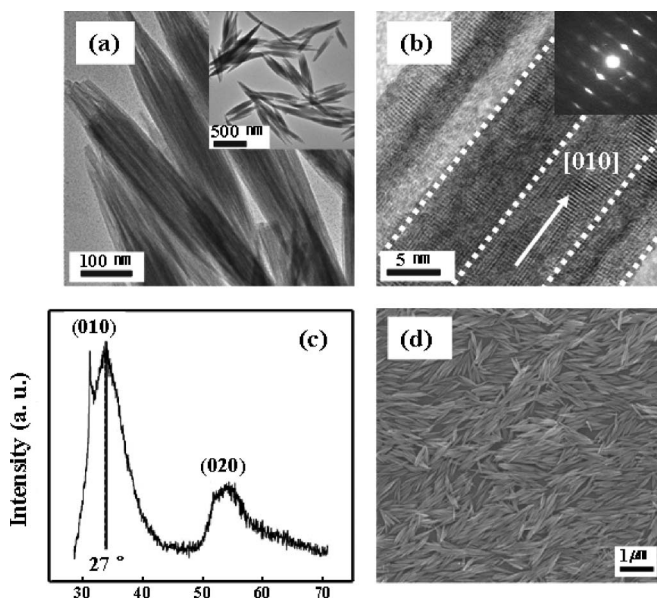


FIG. 1. (a) TEM micrograph of  $\text{WO}_{2.72}$ -NBs. (b) HRTEM micrograph and SAED image taken from each nanobundle. (c) XRD pattern of  $\text{WO}_{2.72}$ -NBs. (d) SEM image of  $\text{WO}_{2.72}$ -NBs deposited on ITO glass by the LB method: the  $\text{WO}_{2.72}$ -NBs films were fabricated in a LB trough with the line force of maximum surface pressure ( $\pi_{\text{max}} = 16.5 \text{ mN/m}$ ).

<sup>a)</sup>Electronic mail: ysung@snu.ac.kr

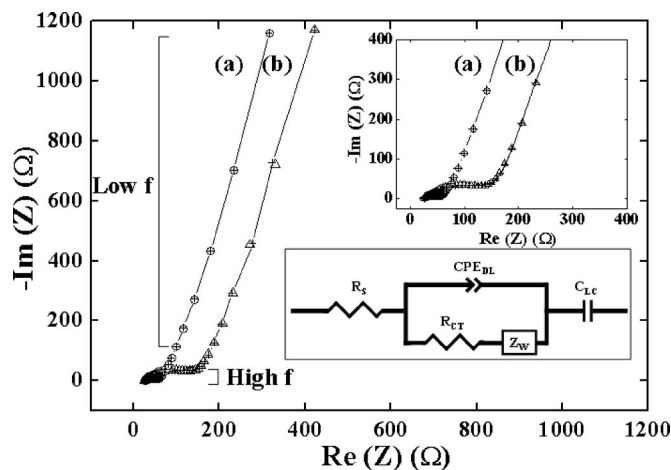


FIG. 2. Nyquist plots of (a)  $\text{WO}_{2.72}$ -NBs (empty circles) and (b)  $a\text{-WO}_3$  (empty triangles) recorded at  $-1$  V vs Ag/AgCl ( $3M$  KCl). Top inset: fit results (crosses). Bottom inset: equivalent circuit.

were synthesized by solvothermal treatment at  $200$  °C for  $10$  h in 1-propanol. As shown in Fig. 1(a), one nanowire bundle is composed of  $15$ – $20$  nanowires  $\sim 6$  nm in diameter and  $\sim 600$  nm in length, and these nanowires are well aligned in one direction in each nanowire bundle. The high-resolution transmission electron microscopy (HRTEM) micrograph indicated that the nanowires grew along the  $[010]$  direction [Fig. 1(b)]. The phase of the nanowire bundle was matched with monoclinic  $\text{W}_{18}\text{O}_{49}$  (or  $\text{WO}_{2.72}$ ),<sup>17</sup> as in the case of our previous study,<sup>15</sup> and the intensities of the  $(010)$  and  $(020)$  peaks were also relatively higher than those of the other peaks. This confirmed that the  $\text{WO}_{2.72}$  nanowires were grown along the  $[010]$  direction, well aligned with the length direction, and self-assembled into nanowire bundles, as shown in the HRTEM result. However, the XRD intensity is not only high in the  $(010)$  plane but also broad at around  $27^\circ$  [Fig. 1(c)]. The angle of approximately  $27^\circ$  corresponded to the  $(012)$ ,  $(311)$ , and  $(211)$  planes of the monoclinic  $\text{WO}_{2.72}$  phase. The selected area electron diffraction (SAED) pattern of one of the nanowire bundles is a diffused spot pattern similar to that of a single crystal [Fig. 1(b), inset]. This indicates that the nanowires in a bundle were well aligned with each other. Hence, the assembly of aligned nanowires caused the increase in the peak intensity of the  $(012)$ ,  $(311)$ , and  $(211)$  planes. Figure 1(d) shows the scanning electron microscopy (SEM) images of the  $\text{WO}_{2.72}$ -NB LB film. The above results obtained from the SEM observations show that the  $\text{WO}_{2.72}$ -NBs have a three-dimensional nematic configuration. When the monolayer of  $\text{WO}_{2.72}$ -NBs is more compressed, it shows a two-dimensional smectic arrangement and, finally, a transition from a monolayer to a multilayer with a three-dimensional nematic configuration was obtained [Fig. 1(d)].<sup>18</sup> It was observed that the  $\text{WO}_{2.72}$ -NBs were partially aligned due to the compression of the layer to produce a quasi-two-dimensional nematic state; however, the overall alignment of the nanowire bundle was imperfect due to the shape of the nanowire bundles.

To determine the  $\text{Li}^+$  diffusion coefficient in the  $\text{WO}_{2.72}$ -NBs and amorphous  $\text{WO}_3$  ( $a\text{-WO}_3$ ) deposited by the sol-gel method,<sup>5</sup> we employed electrochemical impedance spectroscopy. Figure 2 shows the Nyquist plots of the glass/indium tin oxide(ITO)/( $\text{WO}_{2.72}$ -NBs) and the glass/(ITO)/( $a\text{-WO}_3$ ;  $120$  nm thickness) measured at  $-1$  V and the fitting

results obtained using an equivalent circuit model. We varied between  $10$  kHz and  $5$  mHz as a function of the applied frequency. These impedance spectra were analyzed on the basis of the complex nonlinear least-squares fitting method using the equivalent circuit model shown in the inset of Fig. 2. In these circuits,  $R_s$  denotes the electrolyte resistance,  $R_{ct}$  is the charge transfer resistance associated with the ion injection from the electrolyte into the electrochromic electrode,  $Z_W$  is the Warburg diffusion impedance of finite length type, and  $C_{LC}$  is the limiting capacitance.  $\text{CPE}_{DL}$  is a constant phase element describing the distributed capacitance of the electrochemical double layer between the electrolyte and the tungsten oxide.<sup>19</sup> The measured impedance between the electrolyte and tungsten oxide is significantly different for two dimensions ( $\text{WO}_{2.72}$ -NBs: 1D or  $a\text{-WO}_3$ : 2D).  $R_s$  was found to be  $25$ – $26$   $\Omega$  for all of the samples due to the similarity of the electrolyte and cell components. Figure 2 shows the charge transfer resistance at high frequency  $f$  region and diffusion coefficient at low frequency  $f$  region for  $\text{Li}^+$  insertion into the  $\text{WO}_{2.72}$ -NB thin film and  $a\text{-WO}_3$  thin film. The  $\text{Li}^+$  diffusion coefficient of the  $\text{WO}_{2.72}$ -NB thin films was  $1.7 \times 10^{-11}$   $\text{cm}^2/\text{s}$  and that of the  $a\text{-WO}_3$  thin films was  $5.2 \times 10^{-11}$   $\text{cm}^2/\text{s}$ . On the other hand, as is obvious from the displayed spectra, the  $\text{Li}^+$  diffusion coefficient is much higher for the  $a\text{-WO}_3$  thin films than for the  $\text{WO}_{2.72}$ -NB thin films. This phenomenon is due to the short diffusion path of  $\text{Li}^+$  in the case of the  $\text{WO}_{2.72}$ -NBs. The charge transfer resistance of the  $\text{WO}_{2.72}$ -NB thin films was  $28.6$   $\Omega$  and that of the  $a\text{-WO}_3$  thin films was  $146.4$   $\Omega$ . As regards the  $\text{WO}_{2.72}$ -NB thin films, their charge transfer resistance value was remarkably lower than that for the  $a\text{-WO}_3$  thin films. This behavior is associated with the decreased Ohmic polarization of the  $\text{WO}_{2.72}$ -NB thin films during the insertion/extraction of the  $\text{Li}^+$  ions and is explained by their significantly high surface area. The large charge transfer resistance is probably caused by the degradation of the EC device performance. In fact, this is the expected situation that explains the fast ER time and the durability of the EC properties of the 1D nanostructured electrodes during the insertion and extraction processes.

In order to quantitatively compare the electrochromic response time of the  $\text{WO}_{2.72}$ -NB and  $a\text{-WO}_3$ , the difference in transmittance ( $\Delta T$ ) during the coloring/bleaching process was measured, as shown in Fig. 3. All of the electrochemical tests were performed using an Autolab PGSTAT30 potentiostat/galvanostat. Pt, Ag wires, the  $\text{WO}_{2.72}$ -NB LB film, and aqueous  $1M$   $\text{LiClO}_4\text{-PC}$  were used as the counter-electrode, reference electrode, working electrode, and electrolyte, respectively. The transmittance (at  $633$  nm) was simultaneously measured *in situ* during all of the experiments, as described elsewhere.<sup>20</sup> The ER times during the bleaching and coloring processes were calculated on the basis of a 90% transmittance change.

Figure 3 shows the *in situ* normalized transmittance curve obtained during the first cycle of the switched pulse potential test conducted to investigate the coloring/bleaching ER times and transmittance modulation of the  $\text{WO}_{2.72}$ -NBs and  $a\text{-WO}_3$ . The ER times during the bleaching and coloring processes of the  $\text{WO}_{2.72}$ -NBs were about  $1.1$  s and  $3.5$  s, respectively. The ER time of the  $\text{WO}_{2.72}$ -NBs is similar to that reported for organic electrochromic materials ( $<2$  s) (Refs. 21 and 22) and shorter than that of sol-gel deposited  $\text{WO}_3$  films ( $\text{ER}_{\text{bleaching}} = 19$  s,  $\text{ER}_{\text{coloring}} = 27$  s),<sup>5</sup> indicating

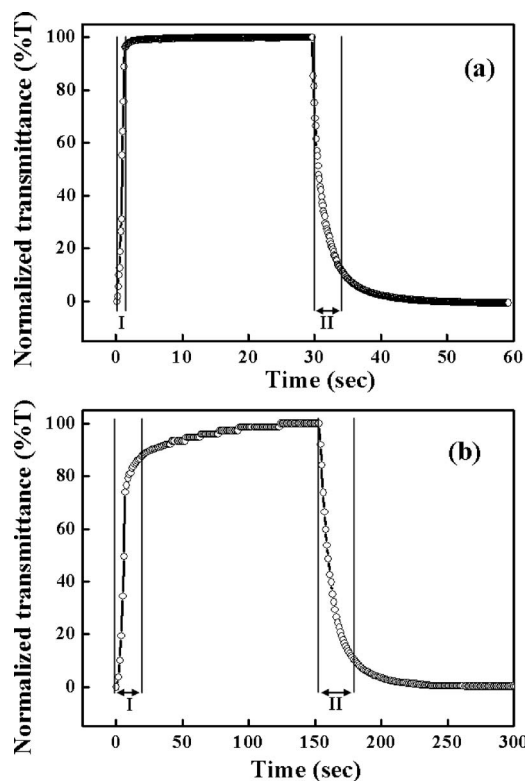


FIG. 3. *In situ* normalized transmittance curve obtained during the switched pulse potential first cycling test performed to measure the coloring/bleaching response times and transmittance modulation of the (a) WO<sub>2.72</sub>-NBs and (b) α-WO<sub>3</sub>.

that the WO<sub>2.72</sub>-NBs have an excellent ER time.

Figure 4 shows the difference in the optical density [ $\Delta OD = \log(T_{\text{bleached}}/T_{\text{colored}})$ ] and coloration efficiency (CE =  $\Delta OD/Q$ ) for the WO<sub>2.72</sub>-NBs and α-WO<sub>3</sub>, where  $Q$  is the charge per unit area participating in the coloring/bleaching process. CE is an important parameter for EC devices. A low CE leads to an irreversible chemical reaction and unwanted side reactions due to the large amount of charge insertion/extraction, which may lead to the degradation of the EC devices. The electrochemical cells of the WO<sub>2.72</sub>-NBs and α-WO<sub>3</sub> had CE values of about 55 and 32 cm<sup>2</sup> C<sup>-1</sup>, respectively, which are comparable to those reported for sputter deposited WO<sub>3</sub> films.<sup>1,2,3</sup> This indicates that the WO<sub>2.72</sub>-NBs have a lower charge insertion/extraction rate, which may result in the enhancement of the long-term stability. The ob-

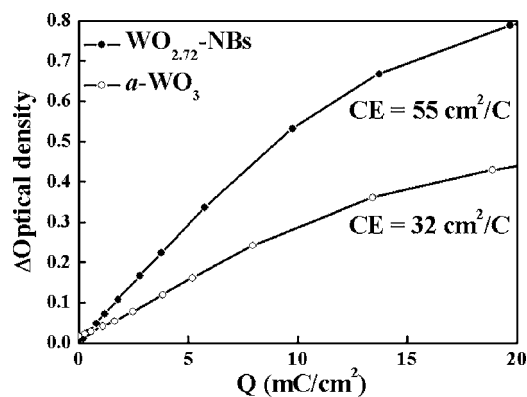


FIG. 4. Plot of *in situ* optical density vs charge density for WO<sub>2.72</sub>-NBs (solid dots) and α-WO<sub>3</sub> (empty circles).

served improved response time and coloration efficiency are due to the high surface area and the short diffusion length for Li<sup>+</sup> at the nanowire-bundle electrode. Although more detailed studies of WO<sub>2.72</sub>-NBs are required, we expect them to be useful as an electrochromic material with a high CE and a good ER time. Detailed studies of this material are currently under way.

In summary, tungsten oxide nanostructures with nanowire-bundle morphology were synthesized via the solvothermal reaction. One nanobundle is a secondary building unit which is composed of 15–20 W<sub>18</sub>O<sub>49</sub> nanowires and is ~6 nm in diameter and ~600 nm in length. Nanobundles with a small size distribution are easily synthesized by the LB method. The WO<sub>2.72</sub>-NBs showed desirable ER times, enhanced reliability, and high CE values. 1D nanostructured tungsten oxide with a large diffusion coefficient and small charge transfer resistance appears to offer high performance EC properties.

Financial support from KOSEF (Grant No. R01-2004-000-10143), the Research Center for Energy Conversion and Storage, the Center for Advanced Materials Processing (CAMP) of the 21st Century Frontier R&D Program funded by the Korean Ministry of Science and Technology, and Brain Korea 21 Program from Korean Ministry of Education is gratefully acknowledged

<sup>1</sup>C. G. Granqvist, *Handbook of Inorganic Electrochromic Materials* (Elsevier, Amsterdam, 1995).

<sup>2</sup>A. Azens, G. Vaivars, M. Veszelei, L. Kullman, and C. G. Granqvist, *J. Appl. Phys.* **89**, 7885 (2001).

<sup>3</sup>K.-S. Ahn, Y.-C. Nah, K.-Y. Cho, S.-S. Shin, J.-K. Park, and Y.-E. Sung, *Appl. Phys. Lett.* **81**, 3930 (2002).

<sup>4</sup>S. J. Yoo, J. W. Lim, and Y.-E. Sung, *Sol. Energy Mater. Sol. Cells* **90**, 477 (2006).

<sup>5</sup>H. Kaneko, S. Nishimoto, K. Miyake, and N. Suedomi, *J. Appl. Phys.* **59**, 2526 (1986).

<sup>6</sup>C. Ho, R. Raistrick, and R. A. Huggins, *J. Electrochem. Soc.* **127**, 343 (1980).

<sup>7</sup>O. Bohnke, M. Rezrazi, B. Vuillemin, C. Bohnke, P. A. Gillet, and C. Rousselot, *Sol. Energy Mater. Sol. Cells* **25**, 361 (1992).

<sup>8</sup>M. S. M. Paul, J. M. Roger, and R. R. David, *Electrochromism: Fundamentals and Applications* (VCH, Weinheim, 1995).

<sup>9</sup>J. Lee, J. Oh, and Y. Tak, *J. Ind. Eng. Chem. (Seoul, Repub. Korea)* **10**, 1058 (2004).

<sup>10</sup>Y. Zhu, H. Li, Y. Kolytyn, Y. R. Hachohen, and A. Gedanken, *Chem. Commun. (Cambridge)* **2001**, 2616.

<sup>11</sup>Z. W. Pan, Z. R. Dai, and Z. L. Wang, *Science* **291**, 1947 (2001).

<sup>12</sup>J. T. Hu, T. W. Odom, and C. M. Lieber, *Acc. Chem. Res.* **32**, 435 (1999).

<sup>13</sup>G. R. Patzke, F. Krumeich, and R. Nesper, *Angew. Chem., Int. Ed.* **41**, 2446 (2002).

<sup>14</sup>K. Lee, W. S. Seo, and J. T. Park, *J. Am. Chem. Soc.* **125**, 3408 (2003).

<sup>15</sup>H. G. Choi, Y. H. Jung, and D. K. Kim, *J. Am. Ceram. Soc.* **88**, 1684 (2005).

<sup>16</sup>A. Tao, F. Kim, C. Hess, J. Goldberger, R. He, Y. Sun, Y. Xia, and P. Yang, *Nano Lett.* **3**, 1229 (2003).

<sup>17</sup>J. Booth, T. Ekström, E. Iguchi, and R. J. D. Tilley, *J. Solid State Chem.* **41**, 293 (1982).

<sup>18</sup>F. Kim, S. Kwan, J. Akana, and P. Yang, *J. Am. Chem. Soc.* **123**, 4360 (2001).

<sup>19</sup>J. R. Macdonald, *Impedance Spectroscopy* (Wiley, New York, 1987).

<sup>20</sup>K. S. Ahn, Y. C. Nah, and Y.-E. Sung, *J. Appl. Phys.* **92**, 1268 (2002).

<sup>21</sup>A. Kumar, D. M. Welsh, M. C. Morvant, F. Piroux, K. A. Abboud, and J. R. Reynolds, *Chem. Mater.* **10**, 896 (1998).

<sup>22</sup>S. I. Cho, W. J. Kwon, S.-J. Choi, P. Kim, S.-A. Park, J. Kim, S. J. Son, R. Xiao, S.-H. Kim, and S. B. Lee, *Adv. Mater. (Weinheim, Ger.)* **17**, 171 (2005).

<sup>23</sup>S. H. Lee, H. M. Cheong, C. E. Tracy, A. Mascarenhas, A. W. Czanderna, and S. K. Deb, *Appl. Phys. Lett.* **75**, 1541 (1999).